

An Isolated Multiport DC - DC Converter for Simultaneous Power Management for PV Application

Meryn Ross Mechery Joseph¹, Jyothi G.K²

¹PG Student, Department of EEE, Federal Institute of Science and Technology, Kerala

²Assistant Professor, Department of EEE, Federal Institute of Science and Technology, Kerala

Abstract: A new isolated multiport dc-dc converter for simultaneous power management of multiple Renewable different sources, which can be of different types and capacities, is designed in this paper. This dc-dc converter only uses one controllable switch in each port to which a source is connected. Therefore, it has the advantages of simple topology and minimum number of power switches. This converter can be also be applied for simultaneous maximum power point tracking (MPPT) control of a wind/solar hybrid generation system consisting of one battery and two different photovoltaic (PV) panels.

Keywords: Isolated dc-dc converter, multiport converter, power management

1. Introduction

In recent years, there has been a growing interest in generating electricity from distributed energy sources. In many applications, it is required to connect multiple energy sources of different types and capacities to a power grid or load. To perform efficient power management and grid integration for the multiple sources, multiport dc-dc converters have been designed. Figure 1.1 shows a multiport dc-dc converter, to which number of sources can be connected. The isolated dc-dc converter has multiple input ports for connecting different sources. The multiport dc-dc converter regulates the low-level dc voltages of the sources to a constant high level required by the inverter.

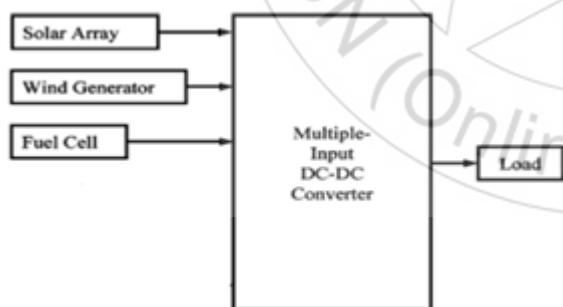


Figure 1.1: Multiport converter

There are two categories of integrated isolated multiport converters. One category of converters uses a transformer with a separate winding for each port. Therefore, all ports are electrically isolated. The other category of converters has multiple ports connected to a single winding on the primary side of a transformer it requires a common ground point for all the input sources. The second topology is preferable due to the advantage of using less number of windings in the transformer. A number of isolated multiport converters belonging to the second category have been proposed.

This paper designs a new isolated multiport dc-dc converter for simultaneous power management of multiple energy sources, where only one switch is used in each input port connected to a source. It does not use any controllable switch on the secondary side of the transformer. Compared with the existing multiport dc-dc converter topologies this converter has the least number of switches and there by a lower cost. This converter is applied for power management of different energy sources.

This paper is organized as follows. The topology of the converter is introduced and the operating principle of the converter is analyzed in Section II. Section III discusses the design considerations for the designed converter. The experimental studies are carried out in Section IV to testify the effectiveness of the designed isolated multiport dc-dc converter for simultaneous control of the different sources. Section VI summarizes this paper with some concluding remarks

2. Designed Isolated Multiport DC-DC Converter

Fig. 2 shows the circuit diagram of the designed isolated multiport dc-dc converter. It consists of a low-voltage side (LVS) circuit and a high-voltage-side (HVS) circuit connected by a high-frequency transformer TX. The LVS circuit consists of m ports in parallel, one energy storage capacitor C_s , and the primary winding of the transformer' each port contains a controllable power switch, a power diode, and an inductor. The HVS circuit consists of the secondary winding of the transformer connected to a full-bridge diode rectifier, and a low-frequency LC filter. The transformer's turn ratio is defined as $n = N_p/N_s$, where N_p and N_s are the numbers of turns of the primary and secondary windings, respectively.

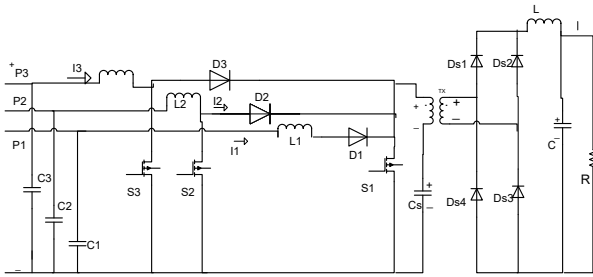


Figure 2: Isolated multiport dc-dc converter

This converter has three operating modes: 1) all switches are on; 2) switch S_1 is off while at least one of the other switches is on; and 3) all switches are off. The equivalent circuits of the converter in the three operating modes are explained below.

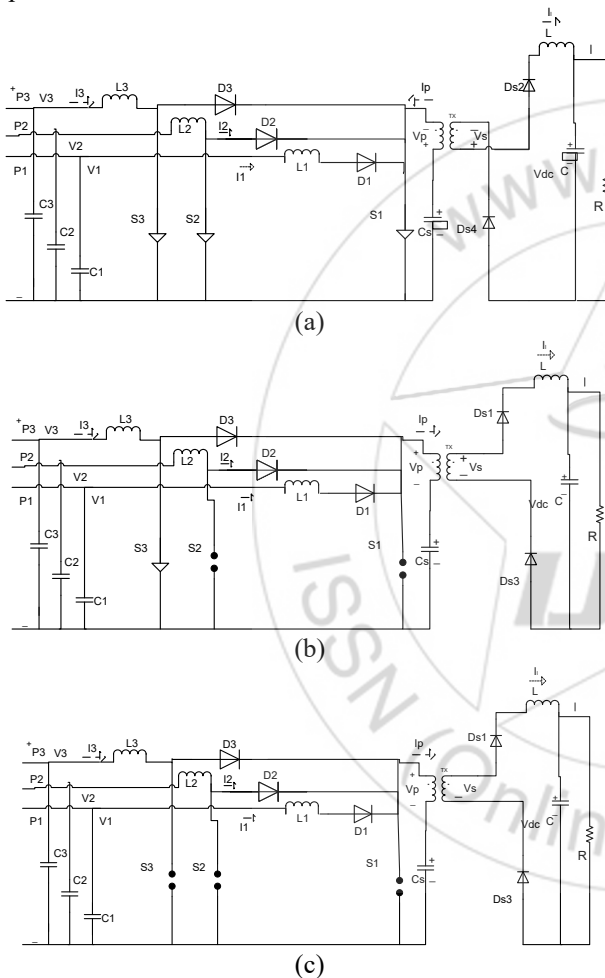


Figure 3: Equivalent circuits of the three operating modes of the designed converter. (a) Mode 1: all switches are on. (b) Mode 2: S_1 is off and at least one of the other switches is on. (c) Mode 3: all switches are off.

MODE 1: $t [t_0, t_1]$ Here all the switches are on and the inductors L_1, \dots, L_m store the energy extracted from the sources; while the energy stored in the capacitor in the previous switching cycle is delivered to the HVS through the diodes D_{s2} and D_{s4} .

MODE 2: $t [t_1, t_3]$ During which S_1 is off and at least one switch S_k ($k = 2, \dots, m$) is on. Here switch S_1 will be off, S_2 will be turned off after some instant and S_k will be on, So here inductor L_1 will be discharging and L_k will be

charging. In mode 2 diodes D_{s1} and D_{s3} will be forward biased.

MODE 3: $t [t_3, t_4]$ Here all the switches are off and all the inductors will be discharging. The operation will be similar as that of mode 2. In mode 3 diodes D_{s1} and D_{s3} will be forward biased.

Figure 4 the steady-state waveforms of the converter in one switching period covering the three operating modes when $m = 3$.

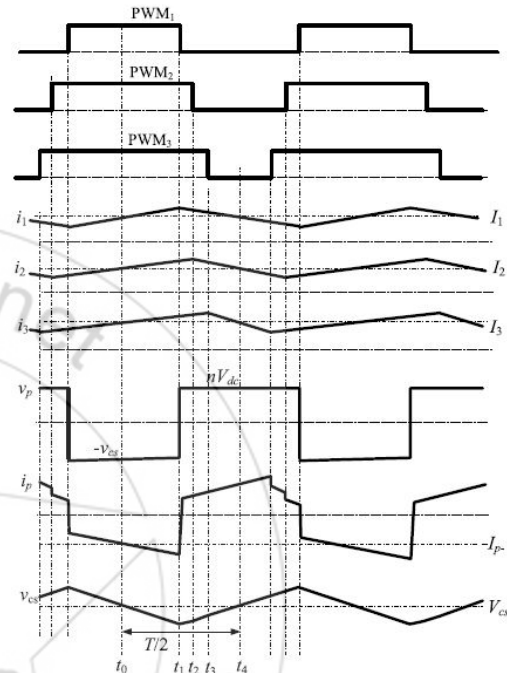


Figure 4: Steady state waveform of the converter

Here we are having three PWM signals. Duty cycle for the switch S_1 should be minimum since first it is turned off. After that the duty cycle of switch S_1 should be minimum and the duty cycle of the switch S_k should be greatest. Here the current i_1, i_2 and i_3 will be charging when the switch is on and will be discharging when the switch is turned off. In mode 1 i_p will be having negative value since it will be owing in reverse direction, in mode 2 the value of i_p will be increasing slowly as the switches are turned off. Similarly in mode 3 the i_p will be increasing and when it again comes to the mode 1 the value of i_p will be slowly increasing as the the switches are turned on.

3. Design Considerations

To make multiple sources work effectively, the following requirement should be satisfied: the switch S_k ($k = 2, \dots, m$) should not be turned off before S_1 is switched off; otherwise, L_k will continuously store energy through S_1 even S_k is off, which is not desired. To meet this requirement, the following inequality should be satisfied for the converter.

$$\min \{d_2, d_3, \dots, d_m\} \geq d_1 \quad (8)$$

Inequality (8) is met if the input voltage of Port 1 (P_1) is the largest, namely the following inequality is satisfied:

$$V_1 \geq \max\{V_2, V_3, \dots, V_m\} \quad (9)$$

where V_k is the output voltage of the k th source ($k = 1, \dots, m$). In practice, the renewable energy source with the largest nominal output voltage will be connected to Port 1. A violation of (9) may lead to one of the following two scenarios.

Scenario 1 (V_1): If no power is available from Port 1, (9) is no longer valid but (8) should still be satisfied. In this scenario, the duty cycle of the switch S_1 is set to be a constant value such that (8) is satisfied, e.g., $d_1 = 0.4$, and the function of the switch S_1 is to change the direction of the current i_p flowing through the transformer. Specifically, when S_1 is off, the current i_p flows from the other sources to the transformer to charge the capacitor C_S . When S_1 is on, the capacitor C_S discharges so that the direction of the current i_p reverses.

Scenario 2 ($0 < V_1 < \max\{V_2, V_3, \dots, V_m\}$): If the maximum power that can be generated by the energy source at Port 1 is low such that (9) cannot be satisfied, (8) should still be satisfied. In this scenario, the duty cycle of the switch S_1 will be increased to a predefined maximum value (e.g., 0.4) by the controller such that (8) is satisfied, and the function of the switch S_1 is the same as that in Scenario 1. In this scenario, the power generated by the energy source connected to Port 1 might be less than the maximum power that can be generated by the source. However, the difference between the generated and the maximum power at Port 1 is small because the maximum available power at Port 1 is usually very low in this scenario. It should be noted that in the aforementioned two scenarios, the sources connected to other ports (i.e., Ports 2– m) can still be controlled simultaneously and independently by appropriately controlling the duty cycles of the corresponding switches. Therefore, in Scenario 1, the power management of all the ports is still independent. In Scenario 2, the power management of Port 1 is not independent, which slightly affects the power generated from Port 1. However, Scenario 2 can be avoided by connecting a boost type voltage regulator between the source and Port 1 so that (9) is always satisfied.

4. PV Modelling

With the advancement in the utilisation of renewable energy, the energy demand can be met with the use of photovoltaic system; a general mathematical description of I-V output characteristics for a PV cell has been studied for over the past four decades. Such an equivalent circuit-based model is mainly used for the MPPT technologies. A solar cell is a p-n junction semiconductor with boron acting as the substrate. Phosphorous atoms are embedded to the boron substrate using high-temperature diffusion method to form the p-n junction. The electrons and holes will contribute for the production of p-n junction. The electrons are stored in semiconductor on two energy bands such as valence band and conduction band. When the photons from the sunlight strikes on the p-n junction surface of the solar cell, the electron-hole combination occurs resulting in the own of charges across the junction by moving some electrons to

conduction band. Some of the charges move towards the valence band. The electrons entering the conduction band result in conduction of current in solar cell. These electrical charges are separated by the potential barrier at the p-n junction. The electrons will move towards the n-type semiconductor and the holes will move towards the p type semiconductor. If the n-type and p-type semiconductors of a solar cell are connected with an external circuit at this moment, the electrons in the n- type semiconductor will move to the other side through the external circuit to combine with the holes in the p-type semiconductor, and then current will. Own through the external circuit, since the output voltage of a solar cell is quiet low that is about 0.5 to 0.7V. The solar cells can be connected in both series and parallel for getting required values of current and voltage from the PV system. The equivalent circuit of the general model which consists of a photo current a diode a parallel resistor expressing a leakage current and a series resistor describing an internal resistance to the current flow as shown in Fig 5.

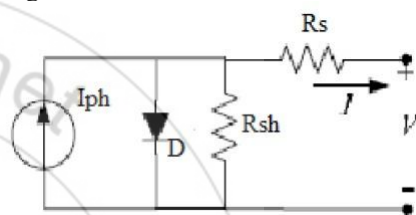


Figure 5: Solar cell model

The voltage-current characteristics equation of a solar cell is given as:

$$I = I_{ph} - \left[\exp\left(\frac{q(V+IR_S)}{KT_C A}\right) - 1 \right] \frac{V+IR_S}{R_{SH}} \quad (1)$$

where I_{ph} is a light-generated current or photo-current, I_s is the cell saturation of dark current, q ($=1.6 * 10^{19}$ C) is an electron charge, k ($=1.38* 10^{23}$ J/K) is a Boltzmann's constant, T_C is the cell's working temperature, A is an ideal factor, R_{sh} is shunt resistance, and R_S is a series resistance of solar cell The photocurrent mainly depends on the solar insolation and cell's working temperature, which is described as

$$I_{ph} = [I_{SC} + K_1(T_C - T_{ref})]H \quad (2)$$

where I_{SC} is the cell's short-circuit current at a 25°C and $1\text{Kw}/\text{m}^2$, K_1 is the cell's short circuit current temperature coefficient, T_{ref} is the cell's reference temperature and H is the solar insolation in Kw/m^2 . On the other hand, the cell's saturation current varies with the cell temperature, which is described as:

$$I_S = I_{RS} \frac{T_C^3}{T_{ref}^3} \exp\left[-\frac{(qE_G)(T_C - T_{ref})}{T_{ref} T_C K A}\right] \quad (3)$$

Where I_{RS} the cell's reverse saturation is current at a reference temperature and standard solar radiation E_{Gh} is the band-gap energy of the semiconductor used in the cell and A is the ideal factor, dependent on PV technology.

A PV array is a group of several PV cells which are electrically connected in series and parallel circuits to generate the required current and voltage. The Simplified terminal equation for the current and voltage of the array becomes as follows:

$$I = N_p I_{ph} - N_p I_s \left(\exp \left(\frac{q(V + I R_{SM})}{K T_C A} \right) - 1 \right) \quad (4)$$

N_p and N_s are number of parallel and series cells.

A generalized PV model is built using Matlab/Simulink according to equations (1),(2)and (4). The simulink model of the above system is given in Fig 6.

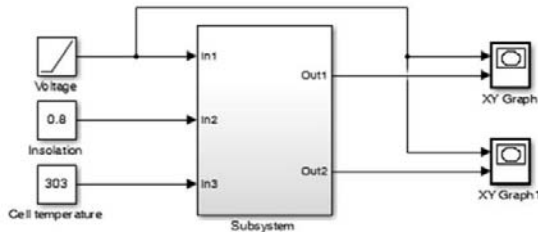


Figure 6: Simulink modal of PV system

The non-linear nature of PV cell is apparent as shown in Fig 7 and 8 ,i.e output current and power of PV cell depend on the cell's terminal operating voltage and temperature ,and solar insolation as well.

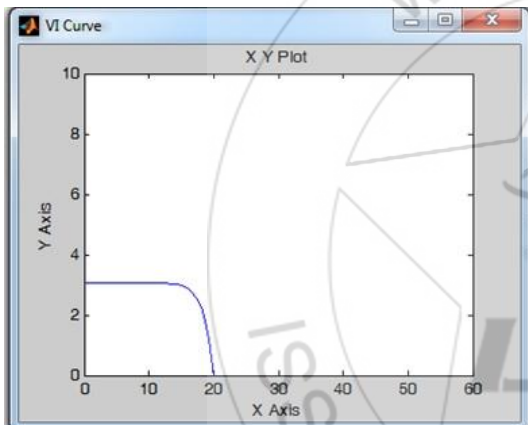


Figure 7: VI graph

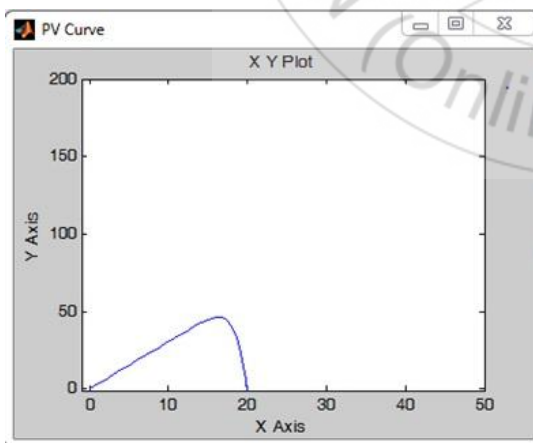


Figure 8: PV graph

With increase of solar insolation, the short circuit current of PV module increases, and the maximum power output increases as well. The reason is that the open circuit voltage is logarithmically depended on solar irradiance, yet the short-circuit current is directly proportional to the radiant intensity.

5. Simultaneous Power Management For A Solar Hybrid Generation System Using The Proposed Converter

In this paper, the proposed converter is applied for MPPT control of a solar hybrid generation system consisting of two PV panels, as shown in Fig. 5. The MPPT controller uses a P&O MPPT algorithm to maximize the output power of the two PV panels simultaneously under various weather conditions. Since the solar radiation and the temperature, the updating frequency of d_1 is set to be the highest. As shown in Fig. 5, the MPPT controller uses the output voltage and current of each source as the input to generate an appropriate pulse width modulated signal for the corresponding switch. The flowchart of the P&O MPPT algorithm is shown in Fig. 5, where $V_{S(k)}$ and $P_{S(k)}$ are the sampled voltage and power of each source at the k th step, respectively, and d is a predefined perturbation value of the switch duty cycle in two consecutive switching periods. The updated duty cycle causes a change in the source current, which leads to the variation of the output power of the source.

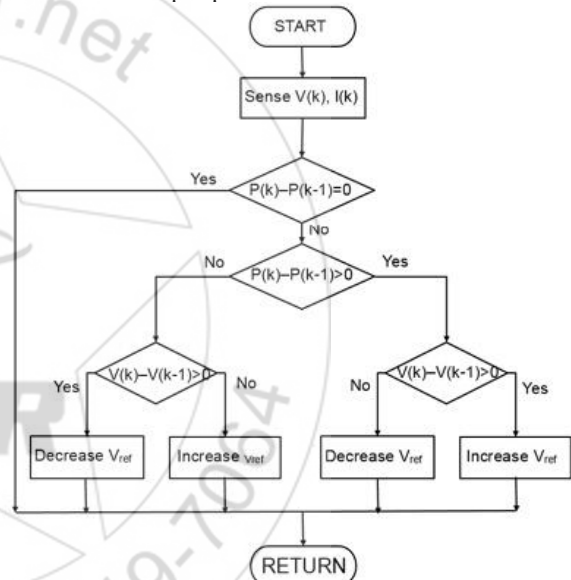


Figure 5: Flowchart of the P&O MPPT algorithm.

6. Experimental Results

With the analysis and design guidelines presented in the previous sections, the designed converter was constructed:

Table 1: Component Specifications of the Converter Constructed

L1	420 μ H	C1-C3	1000 μ H
L2	300 μ H	Cs	1000 μ H
L3	280 μ H	C	1000 μ H
L	1120 μ H	n	7:28
S1	FDP24N40	S2-S3	FDP3632
D1-D3	MUR1510	Ds1-Ds4	EGP50D

The Simulation model of Isolated multiport dc -dc converter is shown below in figure 6 and the converter section is shown in fig 7

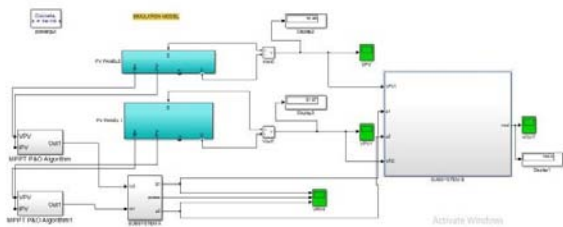


Figure 6: Simulation Circuit of Isolated multiport dc dc converter

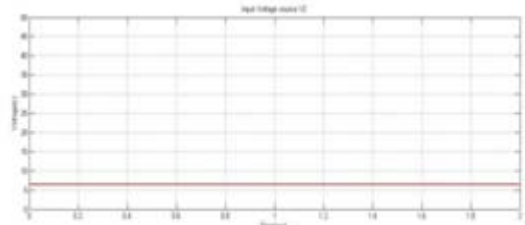


Figure 10: Input voltage of Battery (Source 2)

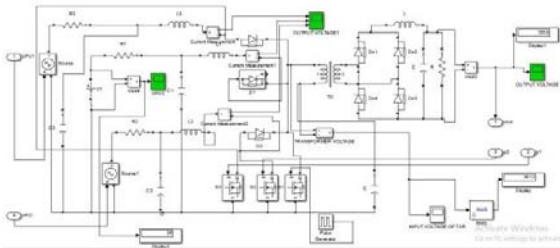


Figure 7: Converter section of Isolated multiport dc dc converter

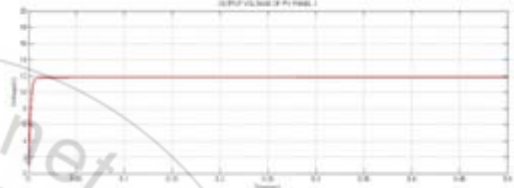
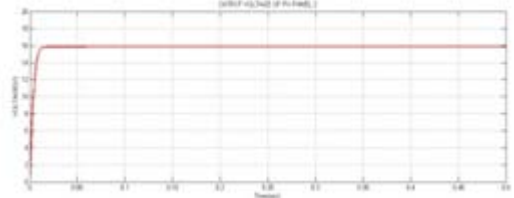


Figure 11: Output voltage of PV panel 1 & 2

Gate pulses to the two PV panels are generated using the circuit given in figure 8. The pulses obtained are shown in figure 9. The pulses for third source i.e. battery is generated by using pulse generator.

Here we are using One battery sources 6.6V and two pv panels, the output of two pv panels is 10.1V AND 11.1V respectively. The output voltage obtained will be a boosted voltage of about 53V in figure 12. Figure 13 shows the output current of two PV panels

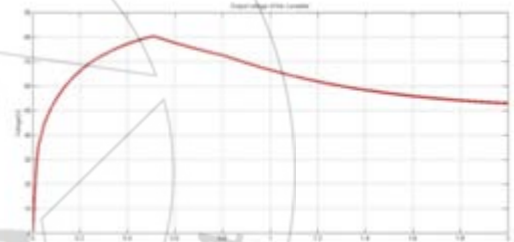


Figure 12: Output voltage of the converter

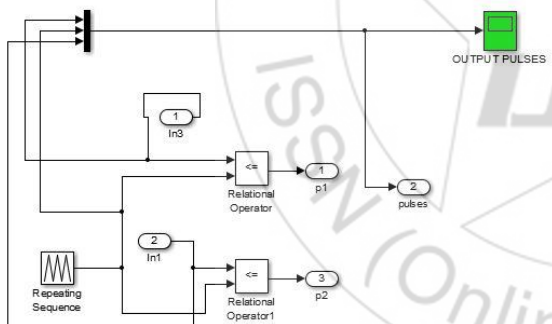


Figure 8: Pulse generation for PV panels

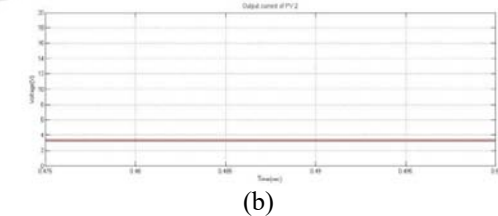
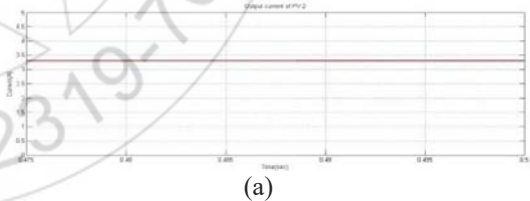


Figure 13: Waveform of output current of PV panels

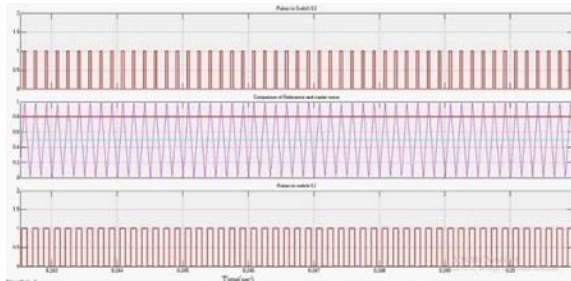


Figure 9: Switching pulses For PV Panels

7. Conclusion

An isolated multiport dc-dc converter that uses the minimum number of switches has been designed for simultaneous power management of multiple energy sources. The designed converter has been applied for simultaneous power management of a three sources. The experimental results have been provided to show the effectiveness of the designed converter. The advantage of

the designed multiport dc-dc converter is its simple topology. Moreover, the designed converter can be easily applied for power management of other types of renewable energy sources.

References

- [1] J. Kassakian and T. Jahns, "Evolving and emerging applications of power electronics in systems," *IEEE J. Emerging Sel. Topics Power Electron.*, vol. 1, no. 2, pp. 47–58, Jun. 2013
- [2] O. Lucia, I. Cvetkovic, H. Sarnago, D. Boroyevich, P. Mattavelli, and F. C. Lee, "Design of home appliances for a DC-based nanogrid system: An induction range study case," *IEEE J. Emerging Sel. Topics Power Electron.*, vol. 1, no. 4, pp. 315–326, Dec. 2013.
- [3] J. Carr, J. Balda, and A. Mantooth, "A high frequency link multiport converter utility interface for renewable energy resources with integrated energy storage," in *Proc. IEEE Energy Convers. Congr. Exposit.*, Sep. 2010, pp. 3541–3548.
- [4] W. Qiao, A. Sharma, J. Hudgins, E. Jones, and L. Rilett, "Wind/solar hybrid generation-based roadway microgrids," in *Proc. IEEE PowerEnergy Soc. General Meeting*, Jul. 2011, pp. 1–7.
- [5] Z. Qian, O. Abdel-Rahman, and I. Batarseh, "An integrated fourport DC/DC converter for renewable energy applications," *IEEE Trans. Power Electron.*, vol. 25, no. 7, pp. 1877–1887, Jul. 2010.
- [6] C. Shen and S. Yang, "Multi-input converter with MPPT feature for wind-PV power generation system," *Int. J. Photoenergy*, Article ID 129254, pp. 129254-1–129254-13, Apr. 2013.
- [7] H. Tao, A. Kotsopoulos, J. Duarte, and M. Hendrix, "Family of multiport bidirectional DC-DC converters," *IEE Proc. Electr. Power Appl.*, vol. 153, no. 3, pp. 451–458, May 2006.
- [8] M. Qiang, Z. Xu, and W. Wu, "A novel multi-port DC-DC converter for hybrid renewable energy distributed generation systems connected to power grid," in *Proc. IEEE Int. Conf. Ind. Technol.*, Apr. 2008, pp. 1–5.
- [9] S. Yu and A. Kwasinski, "Analysis of soft-switching isolated timesharing multiple-input converters for DC distribution systems," *IEEE Trans. Power Electron.*, vol. 28, no. 4, pp. 1783–1794, Apr. 2013.
- [10] J. Zeng, W. Qiao, and L. Qu, "An isolated multiport DC-DC converter for simultaneous power management of multiple renewable energy sources," in *Proc. IEEE Energy Convers. Congr. Exposit.*, Sep. 2012, pp. 3741–3748.
- [11] Q. Li and P. Wolfs, "A review of the single phase photovoltaic module integrated converter topologies with three different DC link configurations," *IEEE Trans. Power Electron.*, vol. 23, no. 3, pp. 1320–1333, May 2008.
- [12] H. Matsuo, T. Shigemizu, F. Kurokawa, and N. Watanabe, "Characteristics of the multiple-input DC-DC converter," *IEEE Trans. Ind. Electron.*, vol. 51, no. 3, pp. 625–631, Jun. 2004.
- [13] Y. Chen, Y. Liu, and F. Wu, "Multi-input DC/DC converter based on the multiwinding transformer for renewable energy applications," *IEEE Trans. Ind. Appl.*, vol. 38, no. 4, pp. 1096–1104, Aug. 2002.
- [14] X. Sun, G. Pei, S. Yao, and Z. Chen, "A novel multi-port DC/DC converter with bi-directional storage unit," in *Proc. Int. Power Electron. Motion Control Conf.*, Jun. 2012, pp. 1771–1775
- [15] C. Zhao, S. Round, and J. Kolar, "An isolated three-port bidirectional DC-DC converter with decoupled power flow management," *IEEE Trans. Power Electron.*, vol. 23, no. 5, pp. 2443–2453, Sep. 2008.
- [16] Z. Zhang, Z. Ouyang, O. Thomsen, and M. Andersen, "Analysis and design of a bidirectional isolated DC-DC converter for fuel cells and supercapacitors hybrid system," *IEEE Trans. Power Electron.*, vol. 27, no. 2, pp. 848–859, Feb. 2012.
- [17] D. Liu and H. Li, "A ZVS bi-directional DC-DC converter for multiple energy storage elements," *IEEE Trans. Power Electron.*, vol. 21, no. 5, pp. 1513–1517, Sep. 2006.
- [18] Z. Wang and H. Li, "Integrated MPPT and bidirectional battery charger for PV application using one multiphase interleaved three-port DC-DC converter," in *Proc. IEEE Appl. Power Electron. Conf. Exposit.*, Mar. 2011, pp. 295–300.
- [19] Z. Wang and H. Li, "An integrated three-port bidirectional DC-DC converter for PV application on a DC distribution system," *IEEE Trans. Power Electron.*, vol. 28, no. 10, pp. 4612–4624, Oct. 2013.
- [20] F. Forest, T. Meynard, E. Laboure, B. Gelis, J. Huselstein, and J. Brandelero, "An isolated multicell intercell transformer converter for applications with a high step-up ratio," *IEEE Trans. Power Electron.*, vol. 28, no. 3, pp. 1107–1119, Mar. 2013.
- [21] G. Su and F. Peng, "A low cost, triple-voltage bus DC-DC converter for automotive applications," in *Proc. IEEE Appl. Power Electron. Conf. Exposit.*, vol. 2, Mar. 2005, pp. 1015–1021.
- [22] Y. Chen, A. Huang, and X. Yu, "A high step-up three-port DC-DC converter for stand-alone PV/battery power systems," *IEEE Trans. Power Electron.*, vol. 28, no. 11, pp. 5049–5062, Nov. 2013.
- [23] F. Blaabjerg and K. Ma, "Future on power electronics for wind turbine systems," *IEEE J. Emerging Sel. Topics Power Electron.*, vol. 1, no. 3, pp. 139–152, Sep. 2013.
- [24] H. Wu, R. Chen, J. Zhang, Y. Xing, H. Hu, and H. Ge, "A family of three-port half-bridge converters for a stand-alone renewable power system," *IEEE Trans. Power Electron.*, vol. 26, no. 9, pp. 2697–2706, Sep. 2011.
- [25] W. Li, J. Xiao, Y. Zhao, and X. He, "PWM plus phase angle shift (PPAS) control scheme for combined multiport DC/DC converters," *IEEE Trans. Power Electron.*, vol. 27, no. 3, pp. 1479–1489, Mar. 2012.
- [26] J. Zeng, W. Qiao, and L. Qu, "A single-switch isolated DC-DC converter for photovoltaic system," in *Proc. IEEE Energy Convers. Congr. Exposit.*, Sep. 2012, pp. 3446–3452.
- [27] Y. Zhao, C. Wei, Z. Zhang, and W. Qiao, "A review on position/speed sensorless control for permanent-magnet synchronous machine-based wind energy conversion systems," *IEEE J. Emerging Sel. Topics Power Electron.*, vol. 1, no. 4, pp. 203–216, Dec. 2013.
- [28] C. Hua, J. Lin, and C. Shen, "Implementation of a DSP-controlled photovoltaic system with peak power tracking," *IEEE Trans. Ind. Electron.*, vol. 45, no. 1, pp. 99–107, Feb. 1998.